Histochem Cell Biol (2016) 145:17–24
DOI 10.1007/s00418-015-1372-9

ORIGINAL PAPER

Aquaporin 2-labeled cells differentiate to intercalated cells in response to potassium depletion

Wan-Young Kim[1] · Sun Ah Nam[1] · Arum Choi[1] · Yu-Mi Kim[1] · Sang Hee Park[2] · Yong Kyun Kim[1,3] · Jin Kim[1]

Accepted: 11 October 2015 / Published online: 26 October 2015

Abstract The mammalian renal collecting duct consists of principal cells (PCs) and intercalated cells (ICs). Both PCs and ICs are involved in potassium (K^+) homeostasis, PCs through their role in K^+ secretion and ICs through their ability to facilitate K^+ resorption. We previously hypothesized that PCs may differentiate into ICs upon K^+ depletion. However, no direct evidence has yet been obtained to conclusively demonstrate that PCs differentiate into ICs in response to K^+ depletion. Here, we present direct evidence for the differentiation of PCs into ICs by cell lineage tracing using aquaporin 2 (AQP2)-Cre mice and R26R-EYFP transgenic mice. In control mice, AQP2-EYFP$^+$ cells exhibited mainly a PC phenotype (AQP2-positive/H^+-ATPase-negative). Interestingly, some AQP2-EYFP$^+$ cells exhibited an IC phenotype (H^+-ATPase-positive/AQP2-negative); these cells accounted for 1.7 %. After K^+ depletion, the proportion of AQP2-EYFP$^+$ cells with an IC phenotype was increased to 4.1 %. Furthermore, some AQP2-EYFP$^+$ cells exhibited a "null cell" phenotype (AQP2-negative/H^+-ATPase-negative) after K^+ depletion. Collectively, our data demonstrate that AQP2-labeled cells can differentiate into ICs, as well as null cells, in response to K^+ depletion. This finding indicates that some of AQP2-labeled cells possess properties of progenitor cells and that they can differentiate into ICs in the adult mouse kidney.

Keywords Aquaporin · Principal cell · Intercalated cells · Differentiation

Introduction

The mammalian renal collecting duct consists of principal cells (PCs) and intercalated cells (ICs), which have different functions and structures (Verlander et al. 1991). Whereas PCs regulate water and sodium balance, ICs maintain the acid–base balance (Wagner et al. 2009).

Both PCs and ICs are involved in potassium (K^+) homeostasis (Giebisch et al. 2003). Specifically, PCs play a role in K^+ secretion and ICs are involved in K^+ reabsorption. Interestingly, K^+ depletion induces adaptive changes in the cellular compositions of both PCs and ICs (Silver et al. 2000). Previous studies have reported that K^+ depletion induces hypertrophy in the inner strip of outer medulla (ISOM) and increases the number and proportion of ICs (Ordonez et al. 1977; Toyoshima and Watanabe 1988; Elger et al. 1992; Bailey et al. 1998; Park et al. 2012). However, it has been unclear whether increase the number and proportion of ICs are due to proliferation of PCs or ICs because the evidence of proliferation was mainly observed in PCs in a previous study (Park et al. 2012). We hypothesized that the conversion of PCs into ICs may be responsible for this

Jin Kim and Yong Kyun Kim have contributed equally to this work.

✉ Yong Kyun Kim
drkimyk@catholic.ac.kr

✉ Jin Kim
jinkim@catholic.ac.kr

[1] Department of Anatomy and Cell Death Disease Research Center, College of Medicine, Bucheon St. Mary's Hospital, The Catholic University of Korea, Banpo-daero 222, Seocho-gu, Seoul 137-701, Korea

[2] Institute of Clinical Medicine Research of Bucheon St. Mary's Hospital, Bucheon-si, Korea

[3] Department of Internal Medicine, College of Medicine, Bucheon St. Mary's Hospital, The Catholic University of Korea, Sosa-ro 327, Wonmi-gu, Bucheon-si, Gyeonggi-do 420-717, Korea

Table 1 Biochemistry after K^+ depletion

	Control	K^+ depletion	*P* values
Kidney weight (g)/Body weight (g), $\times 10^3$	8.0 ± 0.5	12.0 ± 1.4	<0.05
Blood			
K (mmol/l)	4.8 ± 0.8	3.1 ± 0.5	<0.001
Na (mmol/l)	154.1 ± 3.9	155.3 ± 5.1	NS
Urine			
Volume (ml/day)	1.5 ± 0.9	4.1 ± 1.6	<0.001
pH	6.7 ± 0.2	7.2 ± 1.1	<0.05
K (μmol/day)	319.1 ± 85.7	22.4 ± 8.7	<0.001
Na (μmol/day)	290.3 ± 52.0	318.2 ± 63.1	NS
Osmolality (mOsm/kgH_2O)	2217 ± 334	959 ± 149	<0.001
Urinary ammonia excretion (μmol/day)	161.64 ± 9.28	211.76 ± 26.02	<0.05

All values are mean ± SEM

$n = 4$–9/group

increase in ICs (Park et al. 2012). However, no study has yet provided direct evidence for the differentiation of PCs into ICs, especially in adult kidney.

We reasoned that cell lineage tracing using AQP2-Cre mice and R26R-EYFP transgenic mice could conclusively answer whether AQP2-expressing cells can differentiate into ICs. In this study, we generated AQP2-Cre mice and R26R-EYFP transgenic mice and determined the effects of K^+ depletion on their cell populations. After K^+ depletion, the proportion of AQP2-EYFP$^+$ cells with an IC phenotype was significantly increased. Our results shed light on the origin of the increased IC population that arises in response to K^+ depletion, and indicate that AQP2-EYFP$^+$ cells are a type of progenitor cell that can differentiate into ICs.

Materials and methods

Animals

AQP2-Cre mice and R26R-EYFP mice were purchased from The Jackson Laboratory (Bar Harbor, ME, USA). AQP2-Cre mice were crossed with R26R-EYFP reporter mice to generate the AQP2-Cre and R26R-EYFP mouse line. K^+ depletion was performed in AQP2-Cre mice and R26R-EYFP mice (8–12 weeks old, $n = 9$) by feeding mice a K^+-free diet (K^+; 0 gm, Research Diet Inc., New Brunswick, NJ, USA) and distilled water for 14 days. The control group ($n = 7$) was fed a normal diet for 14 days. At the conclusion of the 14-day period, mice were killed and kidney samples were collected. Table 1 shows the biochemistry of K^+ depletion diet. K^+ depletion diet induced hypokalemia with metabolic alkalosis and polyuria, which is consistent with a previous report (Park et al. 2012).

All animal experiments were reviewed and approved by the Animal Care and Use Committee at Bucheon Saint Mary's Hospital, The Catholic University of Korea (License Number: LML13-22). All experiments were performed in accordance with the guidelines for the Principal of Laboratory Animal Care and Use of Laboratory Animals published by the US National Institute of Health (NIH publication, 8th Edition, 2011).

Immunofluorescence analysis and antibodies

Wax-embedded 3-μm sections were processed for multiple immunolabeling studies with anti-H^+-ATPase, anti-EYFP and anti-AQP2 antibodies. Immunofluorescence procedures were performed as previously described (Park et al. 2012). For multiple immunofluorescence experiments, rabbit anti-H^+-ATPase antibodies (Santa Cruz Biotechnology, Santa Cruz, CA, USA) were mixed with chicken anti-EYFP antibodies (Abcam, Cambridge, UK) and goat anti-AQP2 antibodies (Chemicon Inc., Temecula, CA, USA). Labeling was visualized with Alexa 647-conjugated donkey anti-rabbit antibodies (Invitrogen, Grand Island, NY, USA), Cy3-conjugated donkey anti-chicken antibodies (Jackson ImmunoResearch Laboratories Inc, West Grove, PA) and FITC-conjugated donkey anti-goat antibodies (Jackson ImmunoResearch Lab). Tissues were mounted in Vectashield mounting medium (Vector Laboratories). Images were acquired using a Zeiss LSM 510 confocal microscope (Carl Zeiss) and LSM 510 version 2.02 software.

Quantification of labeled cells and statistics

In this study, the ISOM was collected because this duct consists only of PCs and type A ICs. For cell counting, positive (labeled) and negative (unlabeled) cells with a distinct nucleus were included. The number of mice (*N*), images, and cells analyzed for each parameter is listed in Table 2. Values are expressed as percentages of the total numbers of

Table 2 Summary of cell counting

	Control	K^+ depletion
Mouse numbers	4	9
Image numbers	28	63
Number of counted total cells	1695	2550
Average number of counted cell per animal	423.7	283.3

cells and are presented as means ± SDs. Data were compared between groups using an unpaired *t* test; statistical calculations were performed. *P* values less than 0.05 were considered significant.

Results

The number and proportion of ICs increased after K^+ depletion

Both PCs and ICs are involved in K^+ homeostasis, and the cellular composition of two types of cells in collecting duct may change after K^+ depletion. First, we determined whether the numbers and proportions of PCs and ICs are altered in the ISOM by K^+ depletion. Immunofluorescence staining with anti-AQP2 antibodies and anti-H^+-ATPase antibodies revealed that the proportion of ICs (AQP2-negative/H^+-ATPase-positive) was significantly increased (28.3 ± 1.5 vs 33.0 ± 4.5 %) and the proportion of PCs (AQP2-positive/H^+-ATPase-negative) was significantly decreased (71.6 ± 1.5 vs 62.7 ± 5.7 %) after K^+ depletion compared with the control group (Table 3; Fig. 1a).

"Intermediate cells" (AQP2-positive/H^+-ATPase-positive) possess characteristics of both PCs and ICs, whereas "null cells" (AQP2-negative/H^+-ATPase-negative) lack characteristics of either PCs or ICs. These cells were rarely observed in the kidneys from control mice. However, after K^+ depletion, both intermediate and null cells were observed. The proportions of the intermediate and null cells were 1.2 ± 1.1 and 3.0 ± 2.8 % after K^+ depletion, respectively (Table 3; Fig. 2a). These findings are consistent with those reported in our previous study (Park et al. 2012).

Fate of AQP2-labeled cells in the AQP2-Cre and R26R-EYFP adult mouse kidney after K^+ depletion

We previously hypothesized that PCs may be converted into ICs, which could explain the observed increase in ICs in response to K^+ depletion (Park et al. 2012). To determine whether AQP2-labeled cells differentiate into ICs in response to K^+ depletion, we generated an AQP2-Cre and R26R-EYFP mouse line. Kidney sections from these mice were costained with antibodies against EYFP and either AQP2 (to identify PCs) or the H^+-ATPase (to identify ICs).

Table 3 and Fig. 1b show the distribution of AQP2-EYFP$^+$ cells in control mice. Under control conditions, AQP2-EYFP$^+$ cells mainly exhibited the PC phenotype (arrows in Fig. 1b). Interestingly, some AQP2-EYFP$^+$ cells exhibited the IC phenotype; these cells comprised 1.7 ± 0.5 % (arrowheads in Fig. 1b).

Next, the effects of K^+ depletion on the fate of AQP2-labeled cells were determined. Table 3 and Fig. 1a show the distribution of AQP2-EYFP$^+$ cells after K^+ depletion. The

Table 3 Changes of the proportion of PCs, ICs, intermediate cells and null cells after K^+ depletion in inner stripe of outer medulla

	Control (%)		K^+-depletion (%)	
Principal cells (AQP2-positive/H^+-ATPase-negative)				
AQP2-EYFP +	18.3 ± 6.3	71.6 ± 1.5	31.4 ± 8.1*	62.7 ± 5.7*
AQP2-EYFP −	55.3 ± 7.2		30.0 ± 6.1*	
Intercalated cells (AQP2-negative/H^+-ATPase-positive)				
AQP2-EYFP +	1.7 ± 0.5	28.3 ± 1.5	4.1 ± 2.4*	33.0 ± 4.5*
AQP2-EYFP −	26.6 ± 1.4		29.7 ± 4.3*	
Intermediated cells (AQP2-positive/H^+-ATPase-positive)				
AQP2-EYFP +	–	–	–	1.2 ± 1.1*
AQP2-EYFP −	–		1.2 ± 1.1*	
Null cells (AQP2-negative/H^+-ATPase-negative)				
AQP2-EYFP +	0.1 ± 0.1	0.1 ± 0.1	1.3 ± 1.9*	3.0 ± 2.8*
AQP2-EYFP −	–		2.2 ± 0.2*	

Values are expressed as mean ± SD

$n = 4$–9/group

AQP2 aquaporin 2, *EYFP* enhanced yellow fluorescent protein

* Significant different from control mice ($P < 0.05$)

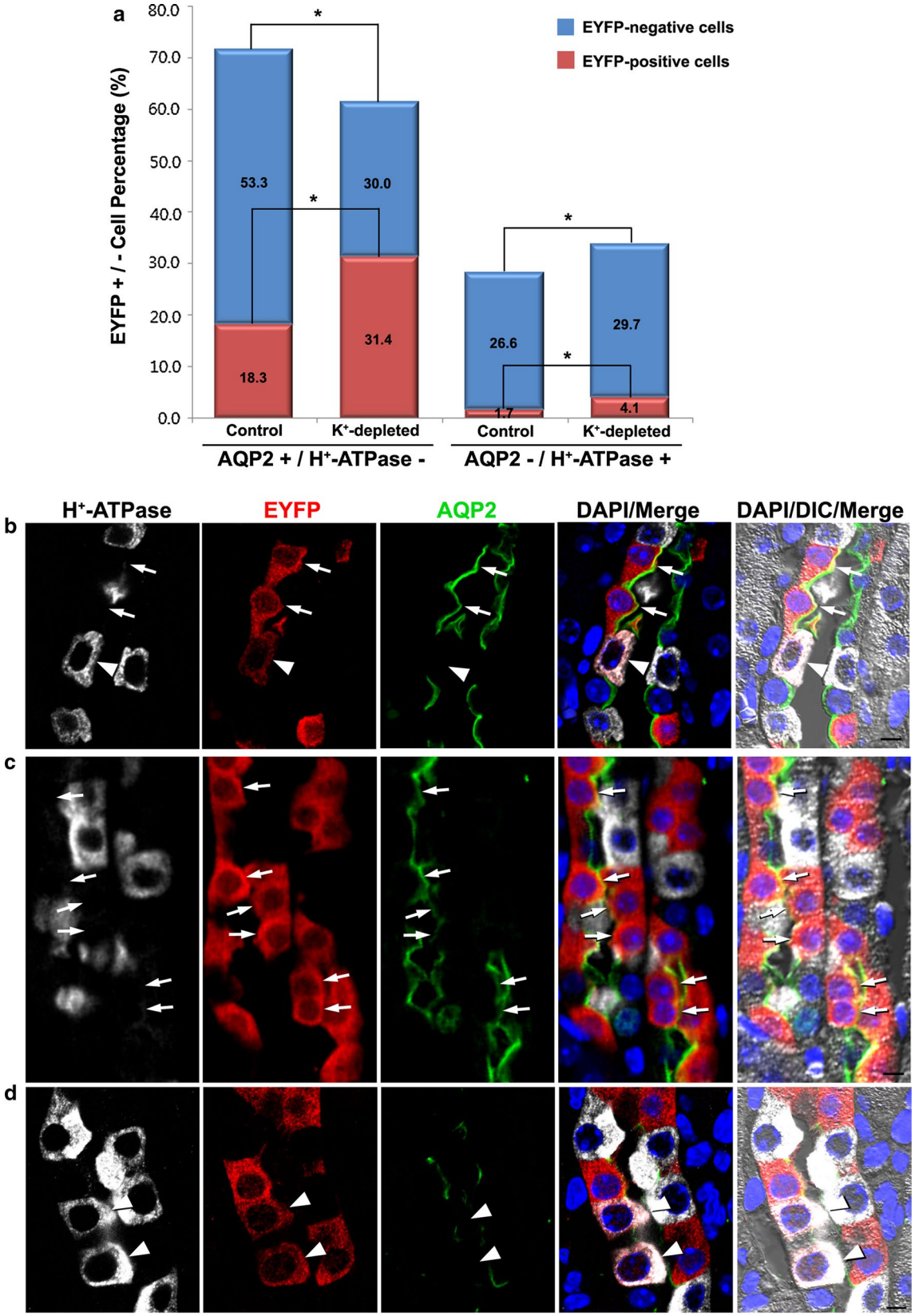
a
EYFP + / - Cell Percentage (%)
80.0
70.0
60.0
50.0
40.0
30.0
20.0
10.0
0.0
EYFP-negative cells
EYFP-positive cells
53.3
18.3
30.0
31.4
26.6
1.7
29.7
4.1
*
Control
K+-depleted
Control
K+-depleted
AQP2 + / H+-ATPase -
AQP2 - / H+-ATPase +
H+-ATPase
EYFP
AQP2
DAPI/Merge
DAPI/DIC/Merge
b
c
d

◀**Fig. 1** Fate of AQP2-labeled cells with phenotype of PCs or ICs after K^+ depletion. **a** Quantification of the proportions of EYFP + or − cells in the collecting duct of inner stripe of outer medulla (ISOM) of the kidneys from control and K^+-depleted AQP2-Cre mice and R26R-EYFP mice. The *bar graphs* indicate the average proportions of PCs (AQP2 +/H^+-ATPase −), ICs (AQP2 −/H^+-ATPase +) per visual field. $*P < 0.05$. **b** Confocal micrographs of 3-μm wax sections of the ISOM of kidneys from control AQP2-Cre mice and R26R-EYFP mice, illustrating immunofluorescence staining for the H^+-ATPase (*white*), EYFP (*red*) and AQP2 (*green*). The merged (with DAPI in *blue*) and DIC images are also shown. Some AQP2-EYFP$^+$ cells exhibited the PC phenotype (*arrows*). Interestingly, some AQP2-EYFP$^+$ cells also exhibited the IC phenotype (*arrowheads*). **c**, **d** In K^+-depleted AQP2-Cre mice and R26R-EYFP mice, the number of PCs with AQP2-EYFP + (*arrows*) and the number of IC with AQP2-EYFP + (*arrowheads*) are increased. *Scale bar* 5 μm

proportion of AQP2-EYFP$^+$ cells with the PC phenotype was significantly increased in K^+-depleted mice compared with control mice (31.4 ± 8.1 vs 18.3 ± 6.3 %, respectively) (arrows in Fig. 1c). Importantly, the proportion of AQP2-EYFP$^+$ cells with the IC phenotype was significantly increased to 4.1 ± 2.39 % in response to K^+ depletion, whereas these cells comprised only 1.7 ± 0.5 % of the population in control mice (arrowheads in Fig. 1d). These findings suggest that AQP2-labeled cells can differentiate into ICs; moreover, some of the ICs that arose in response to K^+ depletion were generated by the differentiation of AQP2-labeled cells into ICs.

We identified intermediate and null cells in K^+-depleted mice. And we analyzed whether AQP2-EYFP$^+$ cells exhibited an intermediate or a null cell phenotype. We observed that the AQP2-EYFP$^+$ cells exhibited a null cell phenotype after K^+ depletion (stars in Fig. 2a, c). Specifically, the proportion of AQP2-EYFP$^+$ cells with null cells phenotype was significantly increased to 1.3 ± 1.9 % in response to K^+ depletion (Table 3; Fig. 2a). However, AQP2-EYFP$^+$ cells with intermediate cells phenotype were not observed after K^+ depletion, while the EYFP$^-$ cells exhibited a intermediate cell phenotype (Table 3; asterisks in Fig. 2b). Our data indicate that AQP2-EYFP$^+$ cells also can differentiate into null cells, which have been proposed to be a type of progenitor/stem cell that can differentiate into ICs (Christensen et al. 2006; Ecelbarger 2006).

Discussion

Although PCs have been proposed to give rise to ICs (Park et al. 2012; Wu et al. 2013), direct evidence from approaches such as cell fate tracing has not yet been obtained to support this hypothesis. Here we performed cell lineage tracing using AQP2-Cre mice and R26R-EYFP transgenic mice to demonstrate that genetically modified AQP2-labeled cells differentiate into ICs in response to K^+ depletion. These findings provide direct evidence that K^+ depletion facilitates differentiation from AQP2-labeled cells into ICs and some of AQP2-labeled cells are progenitor cells that can differentiate into ICs in the adult mouse kidney.

The precise mechanism of differentiation from AQP2-labeled cells to ICs in the response to K^+ depletion is unclear. However, some investigators have suggested plausible explanations. Wu et al. (2013) proposed the hypothesis that AQP2 progenitor cells can differentiated into three cell types: "locked PCs," "locked ICs," and "plastic PCs," and the plastic PCs can give rise to PCs or ICs. They suggested that deletion of *Dot1 l* encoding a methyltransferase specific for histone H3K79 facilitates the differentiation of some of ICs from the plastic PCs. Some investigators demonstrated that forkhead transcription factor Foxi1 regulates the differentiation precursor cells to ICs (Blomqvist et al. 2004; Jeong et al. 2009). Further studies are required to elucidate whether K^+ depletion is associated with these mechanisms in adult mouse kidney.

Beside the differentiation from that AQP2 progenitor cells into ICs, the increased total number of ICs after K^+ depletion may be contributed by the conversion of the type B ICs into the type A ICs, which is modulated by hensin (Schwartz et al. 1985; Fejes-Toth and Naray-Fejes-Toth 1992; Al-Awqati 2008; Gao et al. 2010). However, in our study, cell counting was performed in ISOM, in which no type B ICs have been reported either in control or in K^+-depleted mice. Therefore, we propose that the influence of the conversion of the type B ICs into the type A ICs may be little on increase in total number of ICs after K^+ depletion in this study.

In addition to providing direct evidence of the differentiation of AQP2-EYFP$^+$ cells into ICs, our study also yielded some other interesting findings. First, we found that some AQP2-EYFP$^+$ cells exhibited the IC phenotype in the kidneys from control adult mice, even though the proportion of these cells was small. These findings indicate that some AQP2-EYFP$^+$ cells may not be terminally differentiated in the adult mouse kidney and therefore have the ability to differentiate into ICs as well as PCs, which support the hypothetic model of a previous study that some of AQP2-progenitor cells have plasticity to switch to PCs or ICs (Wu et al. 2013). Second, we found that K^+ depletion led to the appearance of intermediate and null cells, which were not observed in the control adult kidney; moreover, AQP2-EYFP$^+$ cells were responsible for a substantial proportion of the null cells after K^+ depletion. Previous studies reported that null cells were observed upon lithium treatment and that null cells could be considered to be a type of progenitor/stem cell that can differentiate into ICs (Christensen et al. 2006; Ecelbarger 2006). Our data show that AQP2-EYFP$^+$ cells can differentiate into null cells and suggest the possibility that null cells might be able to differentiate into ICs.

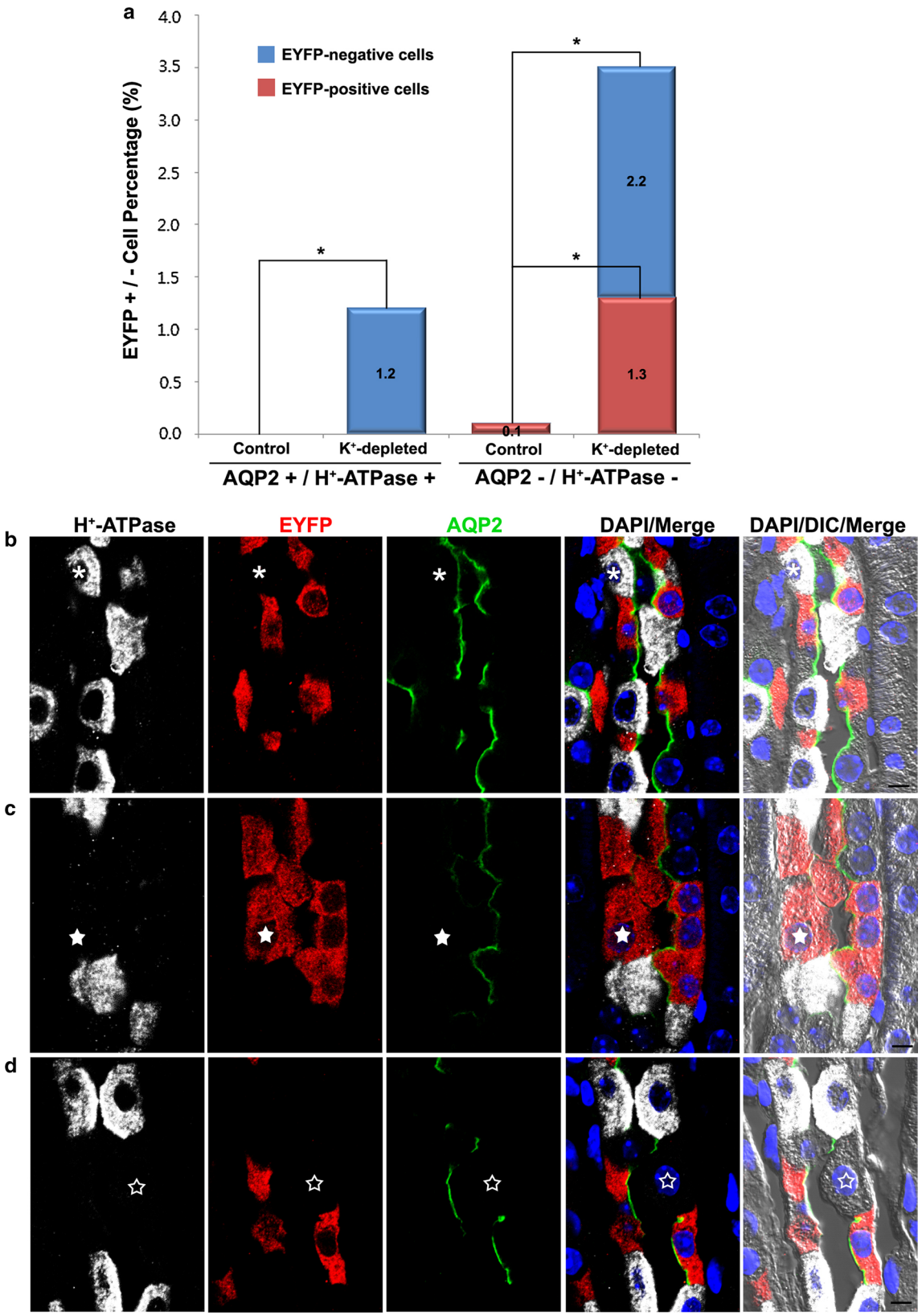
a
EYFP + / - Cell Percentage (%)
4.0
3.5
3.0
2.5
2.0
1.5
1.0
0.5
0.0
EYFP-negative cells
EYFP-positive cells
1.2
2.2
0.1
1.3
*
*
*
Control
K+-depleted
Control
K+-depleted
AQP2 + / H+-ATPase +
AQP2 - / H+-ATPase -
b
c
d
H+-ATPase
EYFP
AQP2
DAPI/Merge
DAPI/DIC/Merge

◀**Fig. 2** Fate of AQP2-labeled cells with phenotype of intermediated or null cells after K^+ depletion. **a** Quantification of the proportions of EYFP + or − cells in the collecting duct of ISOM of the kidneys from control and K^+-depleted AQP2-Cre and R26R-EYFP mice. The *bar graphs* indicate the average proportions of intermediate cells (AQP2 +/H^+-ATPase +), null cells (AQP2 -/H^+-ATPase −) per visual field. *$P < 0.05$. **b**, **d** Confocal micrographs of 3-μm wax sections of the ISOM of kidneys from K^+-depleted AQP2-Cre and R26R-EYFP mice, illustrating immunofluorescence staining for the H^+-ATPase (*white*), EYFP (*red*) and AQP2 (*green*). The merged (with DAPI in *blue*) and DIC images are also shown. Intermediate cells (*asterisks*) are not observed in control kidney but increased in K^+-depleted group. These cells do not have EYFP signals. The number of null cells is increased in K^+-depleted group. Some null cells have EYFP signal (*stars*), and other null cells do not have EYFP signal (*open stars*). *Scale bar* 5 μm

In this study, we observed that only about 18 % of PCs in control mice were AQP2-EYFP-positive in the collecting duct of ISOM, indicating a variegated pattern of transgene activity. Such variegated cellular expression patterns are commonly observed with many transgenes (Robertson et al. 1995; Festenstein et al. 1996). Stricklett et al. (1999) reported similar results that only 40–50 % of inner medullary collecting duct cells were positive for Cre immunoreactivity. Several explanations have been proposed (Nelson et al. 1998), including species specificity of the promoter or the variable presence of enhancers (Wilson et al. 1990), chromatin boundary elements (Felsenfeld et al. 1996) or locus-controlling regions (Festenstein et al. 1996). It suggests that Cre activation among principal cells at baseline was extremely inefficient or that Cre activation itself modifies the response of PCs and/or progenitor cells to K^+-free diet. K^+ depletion increased nearly twofold the % of AQP2-EYFP-positive PCs, while at the same time, K^+ depletion decreased nearly twofold the % of AQP2-EYFP-negative PCs. Thus, the decrease in total number of PCs arises mainly from AQP2-EYFP-negative PCs. Furthermore, it would appear possible that the increment in ICs, intermediate and null cells can be accounted for by the difference between the decrease in AQP2-EYFP-negative cells and the increase in AQP2-EYFP-positive cells. These data suggest also that K^+ depletion strongly activates Cre in those cells in which it has not been activated during development.

In conclusion, our data show that AQP2-$EYFP^+$ cells can differentiate into null cells and suggest the possibility that null cells might be able to differentiate into ICs. This work emphasizes the importance of understanding the differentiation of AQP2-labeled cells after K^+ depletion, and provides new insights into the properties of AQP2-labeled cells as a type of progenitor or stem cell.

Acknowledgments This research was supported by Basic Science Research Program through the National Research Foundation of Korea (NRF) funded by the Ministry of Education, Science and Technology (2013R1A1A2058313) and MRC for Cancer Evolution Research Center (NRF-2012R1A5A2047939).

Compliance with ethical standards

Conflict of interest The authors declare that they have no conflict of interest.

References

Al-Awqati Q (2008) 2007 Homer W. Smith award: control of terminal differentiation in epithelia. J Am Soc Nephrol 19:443–449

Bailey MA, Fletcher RM, Woodrow DF, Unwin RJ, Walter SJ (1998) Upregulation of H^+-ATPase in the distal nephron during potassium depletion: structural and functional evidence. Am J Physiol 275:F878–F884

Blomqvist SR, Vidarsson H, Fitzgerald S, Johansson BR, Ollerstam A, Brown R, Persson AE, Bergstrom GG, Enerback S (2004) Distal renal tubular acidosis in mice that lack the forkhead transcription factor Foxi1. J Clin Invest 113:1560–1570

Christensen BM, Kim YH, Kwon TH, Nielsen S (2006) Lithium treatment induces a marked proliferation of primarily principal cells in rat kidney inner medullary collecting duct. Am J Physiol Renal Physiol 291:F39–F48

Ecelbarger CA (2006) Lithium treatment and remodeling of the collecting duct. Am J Physiol Renal Physiol 291:F37–F38

Elger M, Bankir L, Kriz W (1992) Morphometric analysis of kidney hypertrophy in rats after chronic potassium depletion. Am J Physiol 262:F656–F667

Fejes-Toth G, Naray-Fejes-Toth A (1992) Differentiation of renal beta-intercalated cells to alpha-intercalated and principal cells in culture. Proc Natl Acad Sci USA 89:5487–5491

Felsenfeld G, Boyes J, Chung J, Clark D, Studitsky V (1996) Chromatic structure and gene expression. Proc Natl Acad Sci USA 93:9384–9388

Festenstein R, Tolaini M, Corbella P, Mamalaki C, Parrinngton J, Fox M, Miliou A, Jones M, Kioussis D (1996) Locus control region function and heterochromatin-induced position effect variegation. Science 271:1123–1125

Gao X, Eladari D, Leviel F, Tew BY, Miro-Julia C, Cheema FH, Miller L, Nelson R, Paunescu TG, McKee M, Brown D, Al-Awqati Q (2010) Deletion of hensin/DMBT1 blocks conversion of beta- to alpha-intercalated cells and induces distal renal tubular acidosis. Proc Natl Acad Sci USA 107:21872–21877

Giebisch G, Hebert SC, Wang WH (2003) New aspects of renal potassium transport. Pflugers Arch 446:289–297

Jeong HW, Jeon US, Koo BK, Kim WY, Im SK, Shin J, Cho Y, Kim J, Kong YY (2009) Inactivation of Notch signaling in the renal collecting duct causes nephrogenic diabetes insipidus in mice. J Clin Invest 119:3290–3300

Nelson RD, Stricklett P, Gustafson C, Stevens A, Ausiello D, Brown D, Kohan DE (1998) Expression of an AdsQP2 Cre recombinase transgene in kidney and male reproductive system of transgenic mice. Am J Physio Cell Physiol 275(44):C216–C226

Ordonez NG, Toback FG, Aithal HN, Spargo BJ (1977) Zonal changes in renal structure and phospholipid metabolism during reversal of potassium depletion nephropathy. Lab Invest 36:33–47

Park EY, Kim WY, Kim YM, Lee JH, Han KH, Weiner ID, Kim J (2012) Proposed mechanism in the change of cellular composition in the outer medullary collecting duct during potassium homeostasis. Histol Histopathol 27:1559–1577

Robertson G, Garrick D, Wu W, Kearns M, Marten D, Whitelaw E (1995) Position-dependent variegation of globin transgene expression in mice. Proc Natl Acad Sci USA 92:5371–5375

Schwartz GJ, Barasch J, Al-Awqati Q (1985) Plasticity of functional epithelial polarity. Nature 318:368–371

Silver RB, Breton S, Brown D (2000) Potassium depletion increases proton pump (H(+)-ATPase) activity in intercalated cells of cortical collecting duct. Am J Physiol Renal Physiol 279:F195–F202

Stricklett PK, Nelson RD, Kohan DE (1999) The Cre/loxP system and gene targeting in the kidney. Am J Physiol 276(5 Pt 2):F651–F657

Toyoshima H, Watanabe T (1988) Rapid regression of renal medullary granular change during reversal of potassium depletion nephropathy. Nephron 48:47–53

Verlander JW, Madsen KM, Tisher CC (1991) Structural and functional features of proton and bicarbonate transport in the rat collecting duct. Semin Nephrol 11:465–477

Wagner CA, Devuyst O, Bourgeois S, Mohebbi N (2009) Regulated acid-base transport in the collecting duct. Pflugers Arch 458:137–156

Wilson C, Bellen H, Gehring W (1990) Position effects on eukaryotic gene expression. Annu Rev Cell Biol 6:679–714

Wu H, Chen L, Zhou Q, Zhang X, Berger S, Bi J, Lewis DE, Xia Y, Zhang W (2013) Aqp2-expressing cells give rise to renal intercalated cells. J Am Soc Nephrol 24:243–252